

The modified Williamson-Hall plot and dislocation density evaluation from diffraction peaks

András Borbély*

Mines Saint-Étienne, Univ. Lyon, CNRS, UMR 5307 LGF, F-42023, Saint-Étienne, France

Abstract

Diffraction peak profiles were calculated numerically for dislocation ensembles with different spatial arrangements and correlations between the Burgers vector signs. The latter property determines the stored elastic energy in the crystal and the width of the diffraction peaks. It is shown that [within the approximation of the asymptotic line-profile theory the relationship between peak breadth and the magnitude of the diffraction vector in the *modified* Williamson-Hall \(mWH\) plot is linear](#). The slope of the line is proportional to the arrangement parameter M and to the square root of the dislocation density. The only rigorous way for determining M is the asymptotic Fourier method. Therefore, the evaluation of the dislocation density from the mWH-plot *alone* is impossible and should be avoided. The mWH plot however, is very useful in practice. Its linearity indicates a consistent asymptotic line-profile analysis.

Keywords: Dislocations, X-ray diffraction, Peak broadening, Line Profile Analysis, Dislocation density

X-ray or neutron line profile analysis (LPA) is a powerful tool for determining microstructural parameters such as coherent domain size and dislocation density in faulted crystals [1]. The corresponding theories relate the Fourier transform [2, 3, 4] or the restricted moments [5, 6] of the intensity distribution
5 to parameters of the dislocation ensemble such as the average density (ρ), its

*Corresponding author. e-mail: borbely@emse.fr

spatial fluctuation, and the outer cut-off radius R_e (or the arrangement parameter $M = R_e\sqrt{\rho}$ as introduced by Wilkens [3]). These theories are based on the [mathematical form](#) of the mean square strain ($\langle \varepsilon^2 \rangle$) and have an asymptotic character, which means that the predicted equations describe accurately only
10 the beginning of the Fourier transform or the tail region of the peak profile.

Well before the development of the accurate models, Warren and Averbach proposed a general Fourier method for the evaluation of the coherent domain size and microstrain [7]. This served as starting point for the simplified Williamson and Hall analysis [8] aiming to retrieve the same parameters from the breadths
15 of the peaks. They have shown that for lattice defects creating a Gaussian distribution of atomic displacements, the integral width (β^* , measured in reciprocal space) corresponding to large diffraction vectors (\vec{g}) should be linear as a function of the modulus of $g = 1/d_{hkl}$ ([where \$d_{hkl}\$ is the distance between the planes corresponding to the same \$hkl\$ family](#)). According to their derivation the slope
20 and the intercept of the expected line are proportional to the average microstrain $\langle \varepsilon^2 \rangle^{1/2}$ and to the inverse of the crystallite size ($\sim 1/t$), respectively. Therefore, plotting β^* as a function of g (the so called Williamson and Hall or WH-plot) allows a simple evaluation of these microstructural parameters.

For plastically deformed crystals it was experimentally found that the peak breadths show a characteristic scatter about an imaginary line, a phenomenon called "strain anisotropy" [9]. Based on the results of LPA theories stating that $\langle \varepsilon^2 \rangle$ is proportional to ρ and to the contrast factor C_g of dislocations [10, 11] Ungár and Borbély [12] have introduced modified versions of the Williamson-Hall and Warren-Averbach analyses (called mWH and mWA). Plotting the full width at half maximum (FWHM, which behaves similarly to β^* [11, 13]) as a function of $g\sqrt{C_g}$ the characteristic scatter disappeared in the mWH-plot and the data could be described by a parabola [12]

$$\Delta g_{0.5} = \frac{0.9}{t} + \left(\frac{\pi Ab^2}{2}\right)^{1/2} \rho^{1/2} (g\sqrt{C_g}) + O(g\sqrt{C_g})^2, \quad (1)$$

where $\Delta g_{0.5}$ is the FWHM and 0.9 is the Scherrer factor of a cube shaped
25 crystallite. The parameter A depends on dislocation arrangement (M) and can

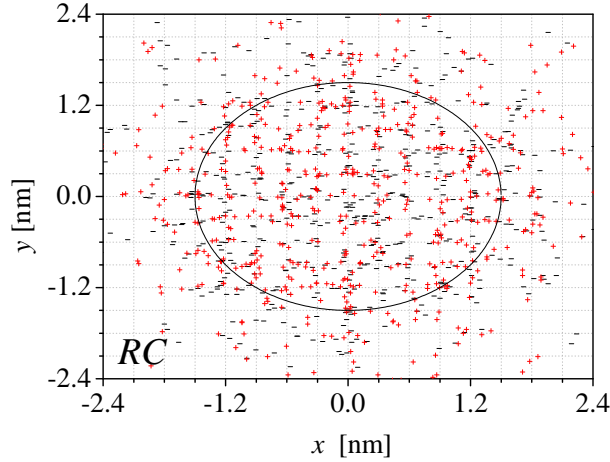
be determined by Fourier analysis only. Nevertheless, the knowlegde of A in eq.(1) could be very useful in practice, since it would allow determining ρ . In spite of its utility and growing interest in using the method (due to its simplicity) no accurate study has been performed revealing the relationship between A and M . According to ref. [14] $A \approx 10$ can be taken for a wide range of dislocation distributions, but [the paper doesn't give](#) more details. In view of the increasing number of publications [15, 16, 17] using the mWH-plot *only* for evaluating ρ , it is important quantifying the relation between A and M as well as the applicability limits of the mWH method.

In this work the peak profiles of infinitely long right circular cylindrical crystals containing screw dislocations parallel to the cylinder axis were numerically calculated by considering the displacement field (\vec{u}) of dislocations for isotropic media [18]. A cylinder radius of $R=1.5 \mu\text{m}$ and a density of $\rho = 10^{14} \text{ m}^{-2}$ were first considered, which resulted in 1424 dislocations in the model (712 inside the cylinder and 712 image dislocations, required by the zero stress condition on the lateral surface of the cylinder [19]). The number of dislocations with positive and negative Burgers vectors was equal and oriented with their senses along $\pm [1, 1, 0]$. The simulations were done considering the fcc lattice of Al with elastic anisotropy close to 1.

To account for correlations between dislocations' spatial position and between their Burgers vectors four arrangements were studied. In the random-random (RR) model both the Burgers vectors and positions were randomly chosen. In the random-cell (RC) model the random Burgers vector choice was kept, but dislocations were positioned into the walls of a cellular structure (fig.1). Finally, random dipoles (RD) and random dipolar cells (RDC) were generated. For these structures the dipole width d , was equal to the average dislocation spacing $\rho^{-1/2} = 0.1 \mu\text{m}$ and the dipole vector sense (\vec{d}) was random. The dipole center locations were randomly chosen over the whole cross section of the cylinder (RD model) or in the dislocation wall region (RDC model).

[In the following we describe the peak profile \$I\(q\)\$ in terms of the reciprocal space variable \$q = k - g\$ with origin at the peak center, where \$k = 2\sin\theta/\lambda\$ is the](#)

Figure 1: Example of a random cell (*RC*) model. Positive and negative dislocations are marked by "+" and "-", respectively. The distance between cell-wall centers in horizontal and vertical directions is $0.3 \mu\text{m}$ and the mean wall thickness is $0.1 \mu\text{m}$.



scattering vector and $g = 2\sin\theta_B/\lambda$ is the diffraction vector corresponding to the peak center given by the Bragg angle θ_B (λ is the wavelength of the X-rays). It is handy to describe $I(q)$ in terms of its Fourier transform

$$A(L) = \int_{-\infty}^{\infty} I(q)e^{-2\pi i q L} dq, \quad (2)$$

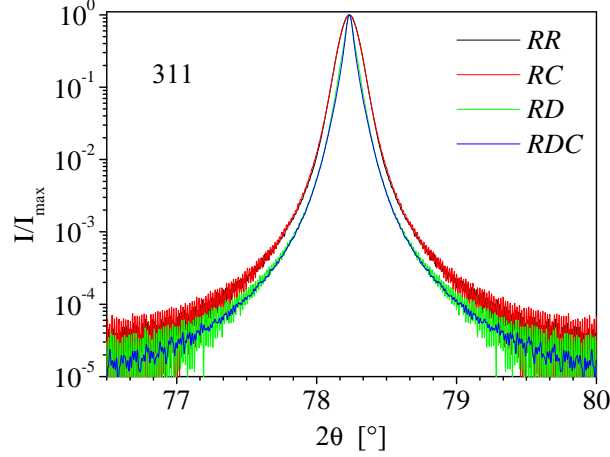
which can be calculated based on the theory of X-ray diffraction [20]. In eq.(2) L is the modulus of the vector \vec{L} perpendicular to the diffracting lattice planes hkl . \vec{L} can be parallel or anti-parallel to \vec{g} . According to the kinematical scattering theory the Fourier transform $A(L)$, of the peak profile for crystals with lattice defects can be written as [3, 10]

$$A(L) = \frac{1}{V} \int e^{2\pi i \vec{g} \cdot [\vec{u}(\vec{r} + \vec{L}) - \vec{u}(\vec{r})]} dV, \quad (3)$$

55 where V is the volume of the crystal and $\vec{u}(\vec{r})$ is the sum of the displacement fields created at point \vec{r} by all the defects in the crystal. Eq.(3) also assumes that diffraction peaks have unit area $\int I(q) dq = 1$.

The real and imaginary parts of the Fourier coefficients (eq.(3)) were calcu-

Figure 2: 311 peak profiles of the studied models. The peaks were calculated for the characteristic radiation $\text{CuK}_{\alpha 1} = 0.15406 \text{ nm}$.



lated by Monte-Carlo integration considering 500,000 random point pairs in the
60 cross section of the cylinder. The imaginary part related to the $\langle \sin \rangle$ term had
values below 10^{-4} in agreement with the negligible polarization of the generated
structures [21] and it was omitted. For each model 100 different configurations
were considered and the Fourier coefficients were averaged. This corresponds to
coherent scattering of the X-rays by all realizations. [The peak profile for a given](#)
65 [model was calculated by taking the inverse Fourier transform of the averaged](#)
[coefficients \(based on eq.\(2\)\).](#) Then the integral breadth (β^*) and the FWHM
were evaluated. β^* was equal to the value obtained from the original coefficients
($\beta^* = 1/(L_1 \sum A(L))$) within a relative error of 10^{-4} , where $L_1 = 3 \text{ nm}$.

Several average peaks were calculated corresponding to the diffraction vec-
70 tors given in Table S1 of the Supplementary Material (SM¹). The 311 peaks
shown in fig.2 indicate that models with uncorrelated Burgers vectors (*RR* and
RC) lead to broader peaks than the models containing dipoles. The latter,

¹ table, figure and equation numbers in the SM are preceded by an S

due to effective screening of their stress fields, create less elastic energy in the crystal and consequently narrower peaks. The original WH-plot of the peaks
75 corresponding to the *RC* model is shown in fig.3. Both β^* and the FWHM follow the linear trend predicted by Williamson and Hall [8]. A characteristic scatter is, however, visible (ex. at equal g) and the non-zero intercepts of the fitted lines suggest the existence of small coherent domains. These "deviations" from the expected line with zero intercept are corrected in the mWH-plot [12] by
80 plotting the widths as a function of $g\sqrt{C_g}$ (fig.4). The corresponding contrast factors are given in Table S1.

Remarkable is the separation of the results in two groups, the *RR* and *RC* models on one side and for *RD* and *RDC* on the other. Since both groups contain models with different spatial arrangements (random and cellular), we
85 conclude that peak broadening and microstrain are mainly determined by the correlation between Burgers vector signs and less by spatial arrangement. The slope and intercept of the fitted lines determine A and the coherent size t (eq.1) and are given in Table 1. Ungár and Tichy [22] have suggested a modification of eq.(1) by plotting $(\Delta g)^2$ as a function of g^2C (see eq. (S3) and fig. S1).
90 The two approaches give identical values for B^2 and A , but there are significant differences between D and t . The corresponding values given in Table 1 indicate that D is smaller than t by a factor of 4 to 7 and is in the range well measurable by standard equipment (below 1 μm). Since no size broadening is expected for the analyzed structures, we conclude that the original formulation (eq.(1))
95 should be used.

The maximum value of $A \approx 1$ is smaller by one order of magnitude than the value of $A = 10$ mentioned in [14]. We emphasize that the *RR* (and also *RC*) model with uncorrelated Burgers vectors corresponds to the upper limit of microstrain created by dislocations, which cannot be realized in real crystals. As
100 shown in ref. [23] uncorrelated dislocations create stored elastic energy which diverges with the crystal size and therefore this model has the largest microstrain. According to discrete dislocation dynamics [24], in plastically deformed crystals a correlation between positive and negative Burgers vectors develops.

Figure 3: WH-plot of the FWHM and β^* for ten peaks corresponding to the *RC* model.

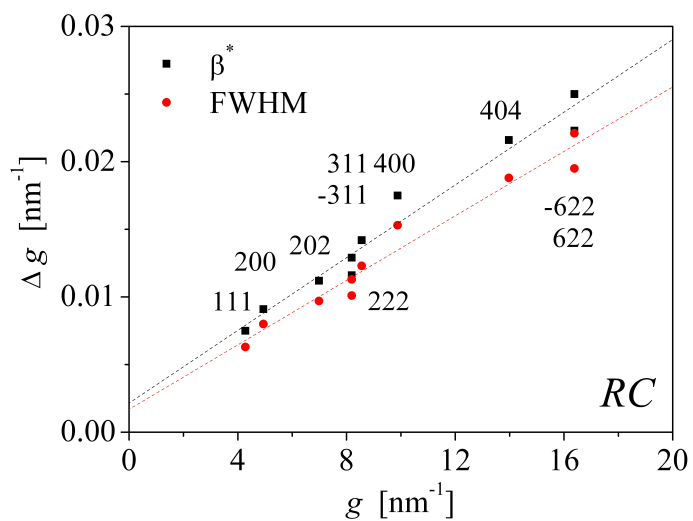


Figure 4: mWH-plot considering the FWHM of 10 peaks corresponding to the studied models.

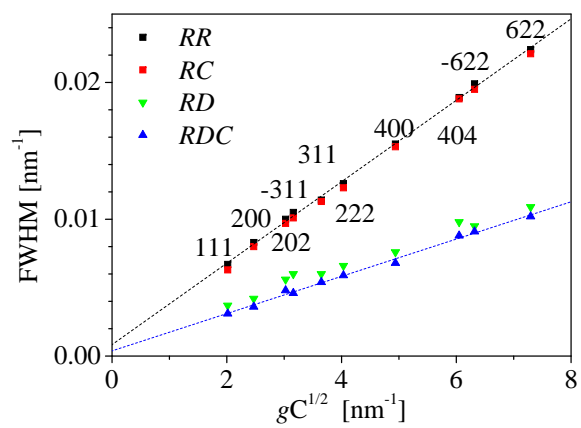


Table 1: Parameters A and t of the mWH eq.(1) as well as B^2 and D after Ungár and Tichy [22] (eq. (S3)). The error of A (and B^2) ≈ 0.02 , while the relative errors of t and D are below 0.01.

<i>Model</i>	<i>RR</i>	<i>RC</i>	<i>RD</i>	<i>RDC</i>
A	0.89	0.87	0.28	0.26
B^2	0.93	0.91	0.30	0.27
t [μm]	1.10	1.19	1.28	4.83
D [μm]	0.26	0.28	0.36	0.66

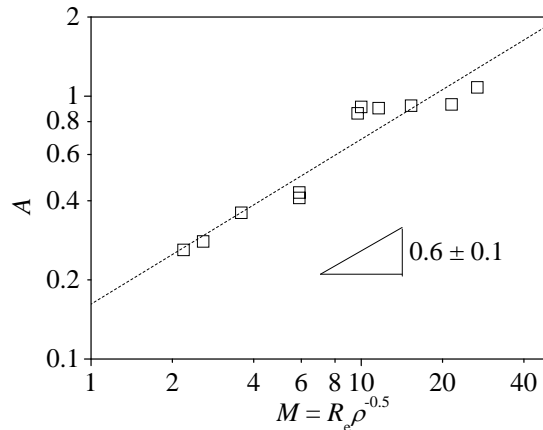
The corresponding correlation length is of about the average dislocation spacing, which means that for real structures $A < 1$. Simulations for edge dislocations (fig. S2) confirmed that the maximum value of $A \approx 1$, which lets us concluding that $A = 10$ [14] underestimates the dislocation density by more than one order of magnitude.

The lower limit of A can be estimated by considering the narrowest dislocation dipoles present in the sample. Using transmission electron microscopy (TEM) Essmann and Mughrabi [25] conclude that the annihilation distance for screw and edge dipoles in copper is of about 50 nm and 1.6 nm, respectively. As this distance can depend on the chemical composition and crystal structure we consider an approximate lower limit for edge dipoles of $d = 5$ nm. Simulations for the RD model give $A \approx 4 \cdot 10^{-6}$, which is practically zero.

According to the above estimations A is between 0 and 1, but the important question which arises is whether one can determine its value in a given experimental case? One possibility would be using TEM, however, the method can be rather time consuming if results with statistical relevance are required. While TEM easily allows determining the spatial arrangement of dislocations, present simulations have shown that peak broadening is mainly determined by the correlations between the signs of the Burgers vectors. At low densities Burgers vector determination is possible by TEM, but it becomes more and more difficult if the local density exceeds a few times 10^{14} m^{-2} .

Evidently, A can be estimated by asymptotic Fourier analysis [2, 3, 4], but

Figure 5: Empirically found relation between A and the Wilkens arrangement parameter M .



in this case the dislocation density and the outer cut-off radius are also obtained, which makes the use of the mWH-plot superfluous for ρ evaluation. For better understanding the asymptotic method it is instructive to recall its basic assumptions and to compare them with the information available in the mWH-plot. The asymptotic Fourier [2, 3, 4] and restricted moment [5, 6] methods exploit the mathematical form of the displacement field of a single dislocation in an infinite medium as well as the approximation that close to the dislocation line the influence of other dislocations on the gradient of \vec{u} is negligible. Thanks to this condition the dislocation density evaluated from the asymptotic models is not affected by the dislocation arrangement. The integral width and the FWHM depend on the contrary on the correlation between the signs of the Burgers vectors over large distances, which in a given practical case is influenced by the crystal structure, deformation path, active slip systems, etc. Fortunately, the Fourier analysis also allows determining the corresponding correlation between the Burgers vector signs, which is expressed in terms of the outer cut-off radius R_e [4] or the M parameter [3]. The asymptotic analysis was performed in this work for all simulated profiles. The results evidence an empirical allometric relationship $A = \alpha M^\beta$, with $\alpha = 0.16 \pm 0.03$ and $\beta = 0.6 \pm 0.1$ (fig.5).

As discussed above there are no means estimating A for a given experimental
145 case other than the Fourier analysis. For this reason the use of the mWH-plot
alone for determining ρ should be avoided. The same remark is also valid for
the phenomenological model of Williamson and Smallman [26] based on the
classical WH-plot. Contrary to its inadequacy for quantitative ρ evaluation,
the mWH plot is very useful in practice for checking the consistency of LPA
150 results. Its main strength relies in the predicted linear relationship between
 β^* (or FWHM) and $g\sqrt{C_g}$. Additional simulations indicate that the second
order term in eq.(1) is negligible for densities varying from 10^{13} to 10^{15} m^{-2}
(fig. S3), for mixed ensembles of edge and screw dislocations (fig. S4) as well as
for the case when dislocations of different slip systems are present. Therefore,
155 when dislocations (or small isotropic coherent domains and dislocations) are
the major sources of peak broadening, the linearity of the mWH-plot suggests a
consistent asymptotic line-profile analysis. This means that the assumptions of
the asymptotic theory were valid and the correct contrast factors were chosen for
the studied case. As an example we consider the case of narrow dipoles ($d = 5$
160 nm), when the mWH-plot is better fitted by a parabola (fig. S5) rather than a
line. In this case the contrast factor (calculated for a single dislocation) fails to
correctly capture the strain field around the dipole, therefore, narrow dipoles
represent an applicability limit of the theory. Such structures have a small M
parameter (≤ 1) [27], which should always raise concern on the validity of the
165 results in real cases.

It seems that the linearity between Δg and g has a much deeper physical
sense than the original approximation of Williamson and Hall [8] for lattice de-
fects creating a Gaussian distribution of atomic displacements. As shown in
ref. [28] this linearity is an intrinsic property of the Bragg equation. Taking
170 its derivative, one can easily show that the peak width $\Delta g = \cos(\theta_B)\Delta(2\theta)$
 $/\lambda$ is linearly related to the standard deviation of the interplanar spacing,
 $< (\Delta d_{hkl}/d_{hkl})^2 >^{1/2}$ (or microstrain) and to the magnitude of the diffrac-
tion vector $g = 2\sin(\theta_B) / \lambda$. Present simulations show that anisotropic effects
induced by the directionality of the displacement field of dislocations as well as

¹⁷⁵ by the non-Gaussian distribution of the atomic displacements are accounted for in the mWH-plot by the square root of the contrast factors.

References

- [1] A. Borbély, T. Ungár, *Comptes Rendus Physique* 13 (2012) 293–306.
- [2] M. Krivoglaz, K. Ryaboshapka, *Fiz. Metallov. Metalloved* 15 (1963) 18–31.
- 180 [3] M. Wilkens, *Fundamental aspects of dislocation theory*, volume 2, U.S. National Bureau of Standards, 1970.
- [4] I. Groma, T. Ungár, M. Wilkens, *Journal of Applied Crystallography* 21 (1988) 47–54.
- [5] I. Groma, *Physical Review B* 57 (1998) 7535.
- 185 [6] A. Borbély, I. Groma, *Applied Physics Letters* 79 (2001) 1772–1774.
- [7] B. Warren, B. Averbach, *Journal of applied physics* 21 (1950) 595–599.
- [8] G. Williamson, W. Hall, *Acta metallurgica* 1 (1953) 22–31.
- [9] P. W. Stephens, *Journal of Applied Crystallography* 32 (1999) 281–289.
- [10] M. Krivoglaz, *Theory of X-ray and Thermal Neutron Scattering by real Crystals* (Plenum Press, NY 1969), Springer-Verlag Berlin Heidelberg New York, 1969.
- 190 [11] M. Wilkens, *Physica status solidi (a)* 2 (1970) 359–370.
- [12] T. Ungár, A. Borbély, *Applied Physics Letters* 69 (1996) 3173–3175.
- [13] A. Borbély, G. Guiglionda, J. H. Driver, *International Journal of Materials Research* 93 (2002) 689–693.
- 195 [14] A. Révész, T. Ungár, A. Borbély, J. Lendvai, *Nanostructured materials* 7 (1996) 779–788.
- [15] R. Renzetti, H. Sandim, R. Bolmaro, P. Suzuki, A. Möslang, *Materials Science and Engineering: A* 534 (2012) 142–146.

- 200 [16] N. Mujica, R. Espinoza, J. Lisoni, F. Lund, et al., *Acta materialia* 60 (2012) 5828–5837.
- [17] B. He, B. Hu, H. Yen, G. Cheng, Z. Wang, H. Luo, M. Huang, *Science* 357 (2017) 1029–1032.
- [18] D. Hull, D. J. Bacon, *Introduction to dislocations*, Elsevier, 2011. doi:10.1016/C2009-0-64358-0.
- 205 [19] J. Eshelby, *Journal of Applied Physics* 24 (1953) 176–179.
- [20] B. Warren, *X-ray Diffraction*, Dover: New York.–1990, 1969.
- [21] I. Gaál, in: *Proc. 5th Riso Int. Symp. on Metallurgy and Material Science*, eds. N. Hessel Andersen, M. Eldrup, N. Hansen, D. Juul Jensen, T. Leffers, H. Lilholt, O. B. Pedersen and BN Singh, Riso National Lab., Roskilde, Denmark, pp. 249–254.
- 210 [22] T. Ungár, G. Tichy, *Physica status solidi (a)* 171 (1999) 425–434.
- [23] M. Wilkens, *Acta Metallurgica* 17 (1969) 1155–1159.
- [24] M. Zaiser, M.-C. Miguel, I. Groma, *Physical Review B* 64 (2001) 224102.
- 215 [25] U. Essmann, H. Mughrabi, *Philosophical Magazine A* 40 (1979) 731–756.
- [26] G. Williamson, R. Smallman, *Philosophical magazine* 1 (1956) 34–46.
- [27] M. Wilkens, *Kristall und Technik* 11 (1976) 1159–1169.
- [28] L. H. Schwartz, J. B. Cohen, *Diffraction from Materials*, Springer-Verlag Berlin Heidelberg, 1987.

